

# STRUCTURE AND MAGNETIC PROPERTIES OF $\text{Fe}_{73.5-x}\text{Ce}_x\text{Cu}_1\text{Nb}_3\text{Si}_{13.5}\text{B}_9$ ALLOYS

Gabriel Pavlík<sup>1</sup>, Pavol Sovák<sup>1</sup>, Vladimír Kolesár<sup>1</sup>, Karel Saks<sup>2,3</sup> and Ján Füzér<sup>1</sup>

<sup>1</sup>Institute of Physics, P.J. Šafárik University, Park Angelinum 9, 04154 Košice, Slovak Republic

<sup>2</sup>Institute of Materials Research, Slovak Academy of Sciences, Watsonova 47, 043 53 Kosice, Slovak Republic

<sup>3</sup>Deutsches Elektronen Synchrotron, Notkestr. 85, 22607 Hamburg, Germany

Received: March 29, 2008

**Abstract.** The aim of this work was to study the influence of iron substitution by Ce in amorphous and nanocrystalline  $\text{Fe}_{73.5-x}\text{Ce}_x\text{Cu}_1\text{Nb}_3\text{Si}_{13.5}\text{B}_9$  ( $x = 3, 5, 7$ ) alloys on their structure and magnetic properties. We present our structural study of amorphous alloys prepared by melt spinning method. Structures of samples were characterized by the X-ray powder diffraction (XRD). The structure stabilities and the structure evolution at a high temperature were addressed by the in-situ XRD experiment in DESY Hamburg. Experimental results confirm the influence of the Ce content on both magnetic and structural properties. Nanocrystalline state of the samples was confirmed by the presence of the ultra-fine  $\text{Fe}_3\text{Si}$  phase. X-ray structure factor and the pair correlation function have been calculated for better characterization of as-quenched samples. Higher content of Ce worsens structural stability of nanocrystalline state and causes crystallization of CeFeSi phase. Magnetic properties reflect the observed structural changes.

## 1. INTRODUCTION

Recently soft magnetic nanocrystalline alloys with ultrafine grains embedded in amorphous matrix have been studied intensively. The most popular alloy system with composition of  $\text{Fe}_{73.5}\text{Cu}_1\text{Nb}_3\text{Si}_{13.5}\text{B}_9$  called FINEMET was in the centre of interest. Many authors tried to improve the soft magnetic properties of Fe-Cu-Nb-Si-B alloys by the substitution of iron by other elements (Mo, Ta, W, Cr, Al) [1-3]. Since the magnetic properties of iron are very sensitive to local environment effects it is expected that the substitution of Fe atoms in Fe-rich alloys by a Rare Earth element would also lead to interesting magnetic phenomena. The aim of this work was to study the influence of annealing treatment and Ce content on structure, magnetic properties and magnetostriction of the  $\text{Fe}_{73.5-x}\text{Ce}_x\text{Cu}_1\text{Nb}_3\text{Si}_{13.5}\text{B}_9$  nanocrystalline ( $x = 3, 5, 7$ ) alloys.

## 2. EXPERIMENTAL PROCEDURE AND DATA ANALYSIS

Amorphous samples of FeCuCeNbSiB were prepared by the melt spinning technique in the form of ribbons. Heat treatments for magnetic measurements were performed in the temperature range of 350 – 600 °C for 1 hour in a vacuum furnace. The saturation magnetization and coercivity were determined from the hysteresis loops traced with fluxmeter in quasi DC magnetic field. Saturation magnetostriction was measured by the so-called small-angle magnetization rotation method.

Two types of high-energy XRD measurements were performed at HASYLAB at DESY on the experimental station BW5 [4] using monochromatic synchrotron radiation of photon energy 100 keV ( $\lambda = 0.124$  keV): The room temperature XRD measurement of as-quenched samples. In situ high-temperature XRD measurement where diffraction

Corresponding author: Gabriel Pavlik, e-mail: gabriel.pavlik@upjs.sk

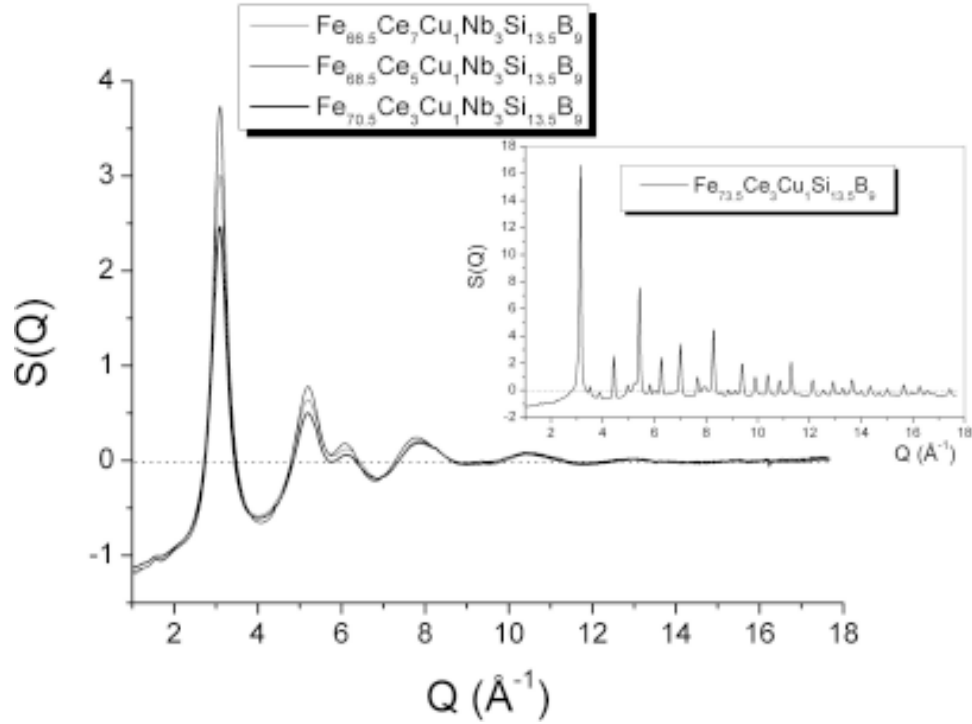


Fig. 1. The total structure factors  $S(Q)$  of rapidly solidified samples.

patterns from the samples were collected in the temperature interval from 300 to 560 °C with 20 °C steps. Both measurements were performed in transmission mode, when the samples were illuminated for 180 s by a well collimated incident beam of 1 mm<sup>2</sup> cross-section and the XRD patterns were recorded using a 2D detector. More details about the experiment are given in [4-6].

According to Faber-Ziman [7] the total structure factor,  $S(Q)$ , can be obtained from the normalized elastically scattered intensity,  $I_e(Q)$  as:

$$S(Q) = \frac{I_e(Q) - \langle f^2(Q) \rangle}{\langle f(Q) \rangle^2}, \quad (1)$$

here

$$\langle f(Q) \rangle^2 = \left( \sum_i c_i f_i(Q) \right)^2, \quad (2)$$

$$\langle f(Q) \rangle^2 = \sum_i c_i f_i^2(Q),$$

the momentum transfer  $Q=4\pi\sin(\theta)/\lambda$ ,  $c_i$  is the concentration of atoms of type  $i$ ,  $f_i(Q)$  is the atomic scattering factor of the element  $i$ . From the  $S(Q)$ 's an atomic pair correlation (distribution) function,  $G(r)$ , can be calculated through a sine Fourier transform as:

$$G(r) = \frac{\rho(r)}{\rho_0} = 1 + \frac{1}{2\pi^2\rho_0} \times \int_{Q_{\min}}^{Q_{\max}} Q(S(Q) - 1) \sin(Qr) dr, \quad (3)$$

here  $\rho(r)$  and  $\rho_0$  is the local atomic and average number density, respectively.

An average coordination number  $N$ , around any given atom in a spherical shell determined by  $r_1$  and  $r_2$  distances can be then calculated as:

$$N = \int_{r_1}^{r_2} 4\pi\rho_0 r^2 G(r) dr. \quad (4)$$

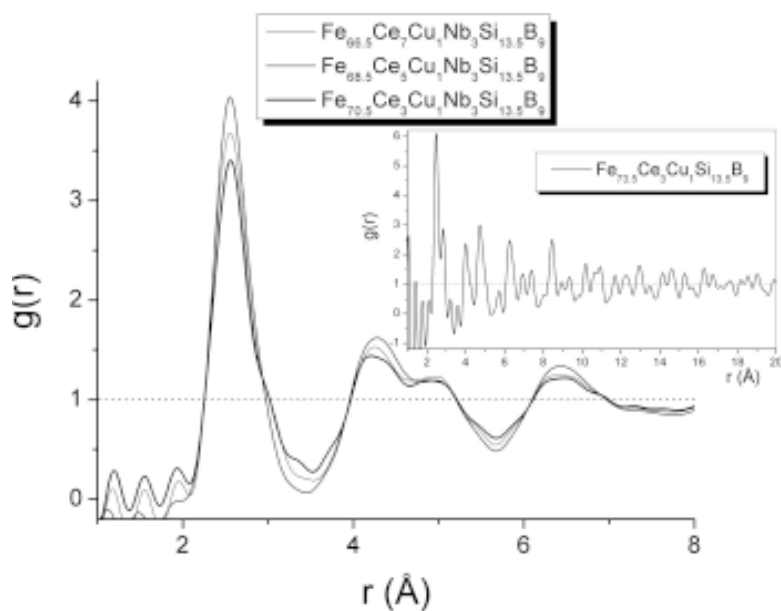


Fig. 2. The pair correlation functions  $G(r)$  calculated from corresponding  $S(Q)$ 's.

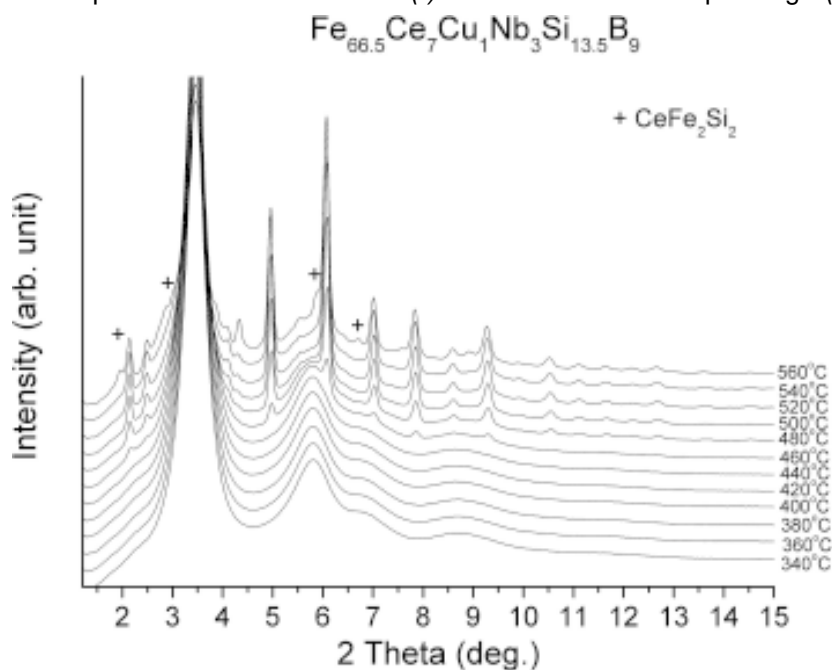


Fig. 3. The XRD patterns of  $\text{Fe}_{66.5}\text{Ce}_7\text{Cu}_1\text{Nb}_3\text{Si}_{13.5}\text{B}_9$  alloy at different stages of annealing.

### 3. RESULTS AND DISCUSSION

#### 3.1. XRD measurements of the as-quenched samples

The total structure factors  $S(Q)$  of rapidly solidified samples are presented in Fig. 1. Samples containing Nb display broad diffuse patterns characteris-

tic for metallic glasses, with a maximum at  $3 \text{ \AA}^{-1}$ . Unlike the six-component samples, the  $S(Q)$  from five-component  $\text{Fe}_{73.5}\text{Ce}_3\text{Cu}_1\text{Si}_{13.5}\text{B}_9$  (insert of Fig. 1) shows intensive Bragg's peaks distributed over the whole  $Q$ -range, what gives us clear evidence that the sample is crystalline. The role of Nb is therefore crucial in the process of the amorphous phase stabilization.

**Table 1.** Magnetic properties of the  $\text{Fe}_{73.5-x}\text{Ce}_x\text{Cu}_1\text{Nb}_3\text{Si}_{13.5}\text{B}_9$  samples.

| Ce content [at.%] | $B_S$ [T] as quenched | $B_S$ [T] $T_A=550$ °C | $\lambda_S$ [ppm] as quenched | $H_C$ [A/m] as quenched | $H_C$ [A/m] $T_A=550$ °C |
|-------------------|-----------------------|------------------------|-------------------------------|-------------------------|--------------------------|
| 3                 | 1,2                   | 1,2                    | 16                            | 48                      | 33                       |
| 5                 | 1,13                  | 1,1                    | 19                            | 36                      | 35                       |
| 7                 | 0,88                  | 0,9                    | 22                            | 31                      | 42                       |

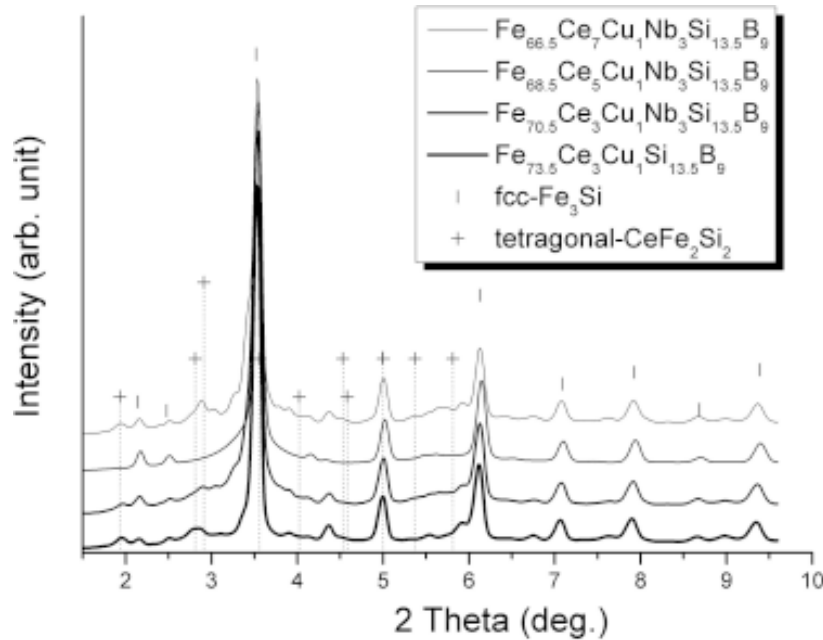
**Fig. 4.** The XRD phase analysis of the samples.

Fig. 2 shows pair correlation functions  $G(r)$  calculated from corresponding  $S(Q)$ 's. These functions show that the main peak has a maximum at  $\sim 2.56$  Å, the value is slightly higher as compared with the Fe-Fe interatomic distance (2.49 Å) reported for the crystalline bcc iron. The shoulder observed at the right side of the main peak  $\sim 3$  Å is a contribution of Ce atoms (the largest atoms in alloy, radius 1.81 Å). It should be also mentioned that the  $\text{Fe}_{68.5}\text{Ce}_5\text{Cu}_1\text{Nb}_3\text{Si}_{13.5}\text{B}_9$  alloy does not show this shoulder. According to our experience [8-10] we suppose, that it could be caused by the fact that the concentration of Ce in this alloy is not homogeneous and might be less than 5 at.%, the value declared by sample producer. Number of atoms in the first shell (between  $r_1=2$  Å and  $r_2=3.43$  Å) of

$\text{Fe}_{73.5}\text{Ce}_3\text{Cu}_1\text{Si}_{13.5}\text{B}_9$ ,  $\text{Fe}_{70.5}\text{Ce}_3\text{Cu}_1\text{Nb}_3\text{Si}_{13.5}\text{B}_9$ ,  $\text{Fe}_{68.5}\text{Ce}_5\text{Cu}_1\text{Nb}_3\text{Si}_{13.5}\text{B}_9$ , and  $\text{Fe}_{66.5}\text{Ce}_7\text{Cu}_1\text{Nb}_3\text{Si}_{13.5}\text{B}_9$  alloys, calculated by Eq. (4), is  $13 \pm 1$ .

### 3.2. High temperature XRD measurements

High temperature XRD measurements proved the significant influence of Ce substitution on the crystallization temperature of the nanocrystalline phase and worsening the stability of obtained nanocrystalline character of the Finemet-based alloys. Fig. 3 shows XRD patterns of the  $\text{Fe}_{66.5}\text{Ce}_7\text{Cu}_1\text{Nb}_3\text{Si}_{13.5}\text{B}_9$  alloy at different stages of annealing. Up to 460 °C the patterns exhibit a broad diffuse modulation characteristic for the amorphous

structure. Already at 460 °C (FINEMET – 500 °C) the XRD pattern shows first diffraction peak which can be indexed as a cubic Fe<sub>3</sub>Si phase (PDF # 42 1329,  $a=5.662$  Å, space group I4/mmm). Intensity of this peak increases progressively with further annealing. At 560 °C a new peak appears as a result of secondary crystallization of Fe<sub>66.5</sub>Ce<sub>7</sub>Cu<sub>1</sub>Nb<sub>3</sub>Si<sub>13.5</sub>B<sub>9</sub> alloy (FINEMET – 650 °C). This peak has a position and relative intensity close to the tetragonal CeFe<sub>2</sub>Si<sub>2</sub> phase (PDF # 40 1268,  $a=3.984$  Å and  $c=9.846$  Å, space group I4/mmm).

XRD patterns obtained for samples pre-annealed at 560 °C and cooled down to room temperature are shown in Fig. 4. Patterns from Fe<sub>73.5</sub>Ce<sub>3</sub>Cu<sub>1</sub>Si<sub>13.5</sub>B<sub>9</sub>, Fe<sub>70.5</sub>Ce<sub>3</sub>Cu<sub>1</sub>Nb<sub>3</sub>Si<sub>13.5</sub>B<sub>9</sub>, and Fe<sub>66.5</sub>Ce<sub>7</sub>Cu<sub>1</sub>Nb<sub>3</sub>Si<sub>13.5</sub>B<sub>9</sub> samples consist of Bragg peaks attributed to at least two phases: cubic Fe<sub>3</sub>Si, tetragonal CeFe<sub>2</sub>Si<sub>2</sub> and a small number of less intense peaks which we were not able to index.

#### 4. CONCLUSION

1. Pair correlation functions  $G(r)$  shows that their main peak has a maximum at  $\sim 2.56$  Å and this shift to higher  $r$  value is caused partially by Fe-Si. This method is sensitive to see the influence of Ce content on  $G(r)$ .
2. It was proved that Ce significantly influences (decreases) crystallization temperature of the nanocrystalline phase and Ce also worsens the stability of obtained nanocrystalline character of the Finemet-based alloys. Ce presence also causes crystallization of the CeFeSi phase and that degrades excellent soft magnetic properties of FINEMET-type alloys.

#### ACKNOWLEDGEMENTS

Authors would like to express their thanks to the Slovak Grant Agency VEGA. The paper was supported by the grant VEGA.

K.S. is indebted to the Slovak Grant Agency for Science for financial support (grant N° 2/7196/27).

#### REFERENCES

- [1] G. Pavlík, P. Sovák, P. Petrovič, A. Zorkovská, P. Matta and M. Konč // *Acta Phys Slovaca* **48** (1998) 675.
- [2] S. Atalay, H.I. Adiguzel, P.T. Squire and P. Sovák // *Mat. Sci. Eng. A* **304-306** (2001) 918.
- [3] A. Zorkovská, P. Petrovič, P. Sovák and J. Kováč // *Czech J Phys* **52** (2002) 163.
- [4] R. Bouchard, D. Hupfeld, T. Lippmann, J. Neufelnd, H. -B. Neumann, H. F. Poulsen, U. Rütt, T. Schmidt, J. R. Schneider, J. Süssenbach and M. von Zimmermann // *J. Synchrotron Rad.* **5** (1998) 90.
- [5] H. Franz, A. Ehnes, A. Roggenbuck, K. Saksl and G. Wellenreuther // *HASYLAB annual report* **1** (2002) 109.
- [6] P. Hammersley, S. O. Svensson, M. Hanfland, A. N. Fitch and D. Häusetmann // *High Press. Res.* **14** (1996) 235.
- [7] T. E. Faber and J. M. Zimman // *Philos. Mag.* **11** (1965) 153.
- [8] A. Zorkovská, J. Kováč, P. Sovák, P. Kollár and M. Konč // *Acta Phys Slovaca* **49** (1999) 449.
- [9] A. Zorkovská, P. Sovák, J.M. Le Breton and M. Kašiarová // *Czech J Phys Suppl. A.* **52** (2002) 137.